Molecular Crystals and Liquid Crystals

ISSN: 1542-1406 (Print) 1563-5287 (Online) Journal homepage: http://www.tandfonline.com/loi/gmcl20

$CuInS_2$-$ZnIn_2S_4$ Solid Solutions: Growth, Physical and Photo-electrical Properties

V. V. Bozhko, A. V. Novosad, G. E. Davidyuk, V. R. Kozer, O. V. Parasyuk, N. Vainorius, A. Sakavičius, V. Janonis & V. Kažukauskas

To cite this article: V. V. Bozhko, A. V. Novosad, G. E. Davidyuk, V. R. Kozer, O. V. Parasyuk, N. Vainorius, A. Sakavičius, V. Janonis & V. Kažukauskas (2014) $CuInS_2$-$ZnIn_2S_4$ Solid Solutions: Growth, Physical and Photo-electrical Properties, Molecular Crystals and Liquid Crystals, 604:1, 164-173, DOI: 10.1080/15421406.2014.968083

To link to this article: http://dx.doi.org/10.1080/15421406.2014.968083

Published online: 15 Dec 2014.

Mol. Cryst. Liq. Cryst., Vol. 604: pp. 164–173, 2014

ISSN: 1542-1406 print/1563-5287 online
DOI: 10.1080/15421406.2014.968083

$CuInS_2$-$ZnIn_2S_4$ Solid Solutions: Growth, Physical and Photo-electrical Properties

V. V. BOZHKO,[1,*] A. V. NOVOSAD,[1] G. E. DAVIDYUK,[1] V. R. KOZER,[1] O. V. PARASYUK,[1] N. VAINORIUS,[2] A. SAKAVIČIUS,[2] V. JANONIS,[2] AND V. KAŽUKAUSKAS[2,*]

[1]Lesya Ukrainka Eastern European National University, Lutsk, Ukraine
[2]Semiconductor Physics Department and Institute of Applied Research of Vilnius University, Vilnius, Lithuania

The horizontal modification of the Bridgman–Stockbarger method was applied to grow the solid solutions of $CuInS_2$-$ZnIn_2S_4$, containing 4 to 16 mol% of $ZnIn_2S_4$. The crystal structure was analyzed by the X-Ray analysis. The induced photoconduction was identified in the single crystals containing 8 to 12 mol% of $ZnIn_2S_4$ by measuring the photocurrent spectra at $T \approx 30$ K. The model of two recombination centers with different capture cross sections was proposed to explain it. Indium vacancies or substitutional defects Cu_{In} were assumed to be the fast recombination centers, meanwhile copper vacancies V_{Cu} behave as the slow recombination centers. The measurements of the temperature dependencies of electrical conductivity and thermally stimulated currents confirmed presence of the electrically active shallow defects in these n*-type samples.*

Keywords Inorganic solid solutions; crystal growth; crystal structure; semiconductors; photoconductivity; defects

1. Introduction

The ternary $CuInS_2$ compound has the chalcopyrite structure and is promising for optoelectronic applications, e.g., for the fabrication of high efficiency thin film Solar cells [1–3]. Its direct optical gap of about 1.55 eV is optimally placed relative to the maximum in the solar spectrum. It has high chemical and thermal stability that make $CuInS_2$ a very attractive material for fabricating cheap and efficient solar elements [4, 5]. Advances of modern electronics require development of semiconducting materials with precisely controllable properties. The promising way is, for instance, a purposeful combination of the traditional materials with similar structure in the solid alloys. The accurate control of the material compositions enables the smooth variation of their optical and electrical properties. In this work solid alloys $CuInS_2$-$ZnIn_2S_4$ with 4, 8, 12, and 16 mol% $ZnIn_2S_4$ were investigated. They had n-type electrical conductivity. Unfortunately, the samples with as much as 16 mol% of $ZnIn_2S_4$ were the two-component ones. The X-Ray structural analysis was used to reveal the microscopic structure of the samples.

*Address correspondence to V. V. Bozhko, Lesya Ukrainka Eastern European National University, av. Voli 13, Lutsk 43025, Ukraine. E-mail: bozhko@univer.lutsk.ua

Color versions of one or more of the figures in the article can be found online at www.tandfonline.com/gmcl.

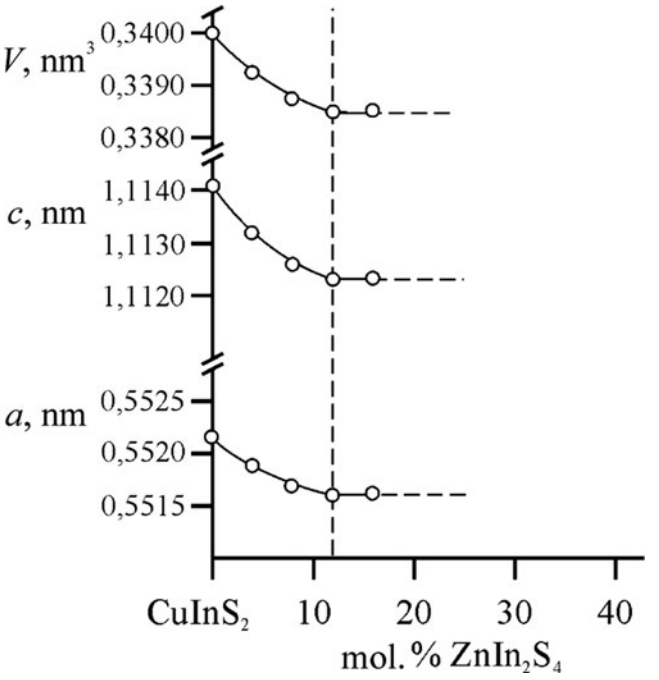

Figure 1. Parameters of the elementary cells of the $CuInS_2$–$ZnIn_2S_4$ solid solutions depending on $ZnIn_2S_4$ content.

2. Results and Discussion

To find the regions of solid-phase solubility in the system $CuInS_2$-$ZnIn_2S_4$ five series of samples with different contents of $ZnIn_2S_4$ were prepared. High-purity elements (with a purity grade not less than 99.99 wt.%) were used for synthesis. The evacuated quartz ampules with the blends were placed into the furnace and heated up to 720 K. They were kept at this temperature for 48 hours in order to assure the maximum binding of elemental Sulfur. Afterwards the ampules were heated up to 1470 K, and were kept at this temperature for 1 hour. Later on they were cooled with a rate of 10–15 K per hour down to the annealing temperature of 870 K. The annealing lasted for 500 hours and was followed by the quenching in cold water. The obtained samples were analyzed by the powder X-ray diffraction (XRD), using the CuK_α radiation diffractometer ДРОН 4–13.

The elementary cell parameters were calculated using the CSD software [6]. The solid-solution ranges were determined by analyzing variation of the elementary cell parameters (Fig. 1). It can be seen that solid solubility of $ZnIn_2S_4$ in the low temperature modification of $CuInS_2$ with chalcopyrite structure can be achieved in the ranges of 0–12 mol% $ZnIn_2S_4$ at the annealing temperature.

To study the mechanism of formation of the investigated solid solutions, we used the X-ray diffraction analysis. As an example, the experimental, calculated and differential diffraction patterns in the solid compound $Cu_{3.14}Zn_{0.43}In_4S_8$ (12 mol% $ZnIn_2S_4$) are shown in Fig. 2. In 4*a* (0,0,0) crystallographic position the heterovalent substitution of Cu atoms by Zn atoms was found with one divalent Zn atom replacing two univalent Cu atoms. As the tetrahedral radii of Cu^+ and Zn^{2+} ions are very similar (~ 0.074 nm [7]), thus the substitution reaction can be written as $2Cu \leftrightarrow Zn + \square$, here $\square$ represents the tetrahedral cavity. So, the

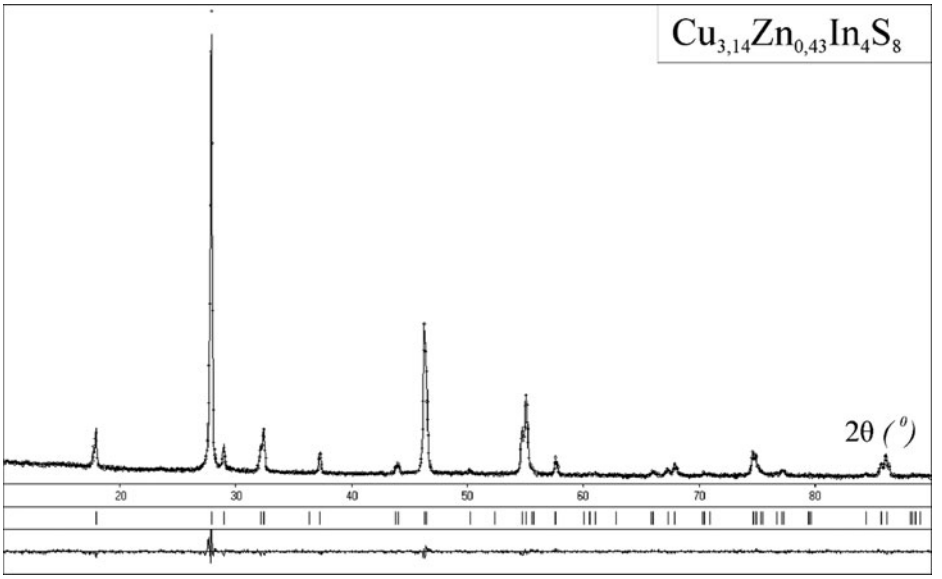

Figure 2. Experimental, calculated and differential diffraction patterns in the solid compound $Cu_{3.14}Zn_{0.43}In_4S_8$ (12 mol% $ZnIn_2S_4$).

vacancy type cationic defects within the chalcopyrite structure are formed, the density of which is proportional to the density of Zn atoms. Hence, one can expect that properties of the material would be affected by cation vacancies, which are not observed in the chalcopyrite $CuInS_2$ structure., as, e.g., in Ref. [8]. This leads to the reduction of the elementary cell dimensions with growing content of $ZnIn_2S_4$ (Fig. 1), i.e., compression of the tetrahedral cavities because of the lack of metal atoms in them. Crystallographic positions of the atoms and the interatomic distances in the solid compound $Cu_{3.14}Zn_{0.43}In_4S_8$ (12 mol% $ZnIn_2S_4$) are presented in Tables 1 and 2.

A horizontal version of the Bridgman–Stockbarger method was chosen for the solid solution crystal growth. Initial compositions were selected within the homogeneity range of the solid solutions at 870 K (Fig. 1). The polycrystalline ingots preliminary synthesized from high-purity elements (better than 99.99 wt%) and weighting 8 g were sealed in evacuated quartz ampoules with conic ends and placed in a two-zone furnace inclined at an angle of 15^0.

The technological data and equipment structure are described in detail in [9, 10]. Both zones have independent temperature control and can be translated along the growth axis via a lead screw connected to a motor. The ampoule was fixed on a quartz rod and centered in the furnace tube. The longitudinal temperature profile was measured with an external thermocouple.

After heating to 1470 K, the melts were homogenized for 4 h by rotating the ampules with the attached quartz rod. Afterwards translation of the furnace was started at a rate of 1 cm/day, by keeping the ampule stable. The temperature gradient at the crystallization front did not exceed 14 K/cm, assuming that the gradient at the interface is similar to the temperature profile of the furnace. After reaching the isothermal zone at 870 K, the crystals were annealed for 250 h and then cooled down to room temperature at a rate of 100 K/day. As a result, we obtained boules consisting of single crystal blocks, with dimensions suitable

Table 1. Crystallographic positions (CP), Crystallographic occupation factors and the Isotropic parameters of the atoms in the solid compound $Cu_{3.14}Zn_{0.43}In_4S_8$ (12 mol% $ZnIn_2S_4$)

Atom	CP	*x*	*y*	*z*	Crystallographic occupation factors	Isotropic parameters $B_{iso} \times 10^2$, nm^2
M1	4*a*	0	0	0	0.79Cu+ 0.11Zn+ 0.11□	1.16(9)
In	4*b*	0	0	1/2	1	1.24(5)
S	8*d*	0.2228(9)	1/4	1/8	1	0.99(10)
Elementary cell parameters: $A = 0.55164(2)$ nm $c = 1.11229(7)$ nm $V = 0.33848(5)$ nm^3						

for physical experiments (Fig. 3). Energy-dispersive X-ray spectroscopy (EDX) was used to analyze the composition of the grown crystals. Concentrations of each element are given in Table 3. The compositions are close to that predicted in advance. Absence of Zn in the crystal with 4 mol% $ZnIn_2S_{4-}$ is probably caused by the low concentration of it.

Electrical measurements were carried out using the specimens fabricated in the form of regular parallelepipeds (3–8)*(0.5–1)*(1–2) mm^3 in size. The samples surfaces were mechanically polished using diamond pastes with various granular sizes. The indium or gallium-indium eutectic mixture contacts were attached to the samples. They were ohmic at the voltages used. To analyze defect spectra and their activation energies spectral dependencies of the crystal photoconductivity were measured at ∼ 30 K. The spectra were scanned in two opposite directions. First, they were measured by increasing quantum energy from 0.5 eV up to 2.5 eV. Later on, to reveal effects of the light excitation, spectra were scanned in the opposite direction.

To assure stationary excitation conditions, durations of the single scans were as long as 2600 s. In Fig. 3(a) spectral dependencies of photoconductivity of the $CuInS_2$-$ZnIn_2S_4$ crystals with 4 mol% of $ZnIn_2S_4$ are shown. In these crystals photoconductivity maxima appear at the same position of ∼1.52 eV by both scan directions, and might be attributed to

Table 2. Interatomic distances (δ) and the coordination numbers (CN) in the solid compound $Cu_{3.14}Zn_{0.43}In_4S_8$ (12 mol% $ZnIn_2S_4$)

Atom		*δ, nm*	CN
M1 2M1	−4S	0.2312(3)	4
In	−4S	0.2485(3)	4
S	−2M1	0.2312(3)	4
	−2In	0.2485(3)	

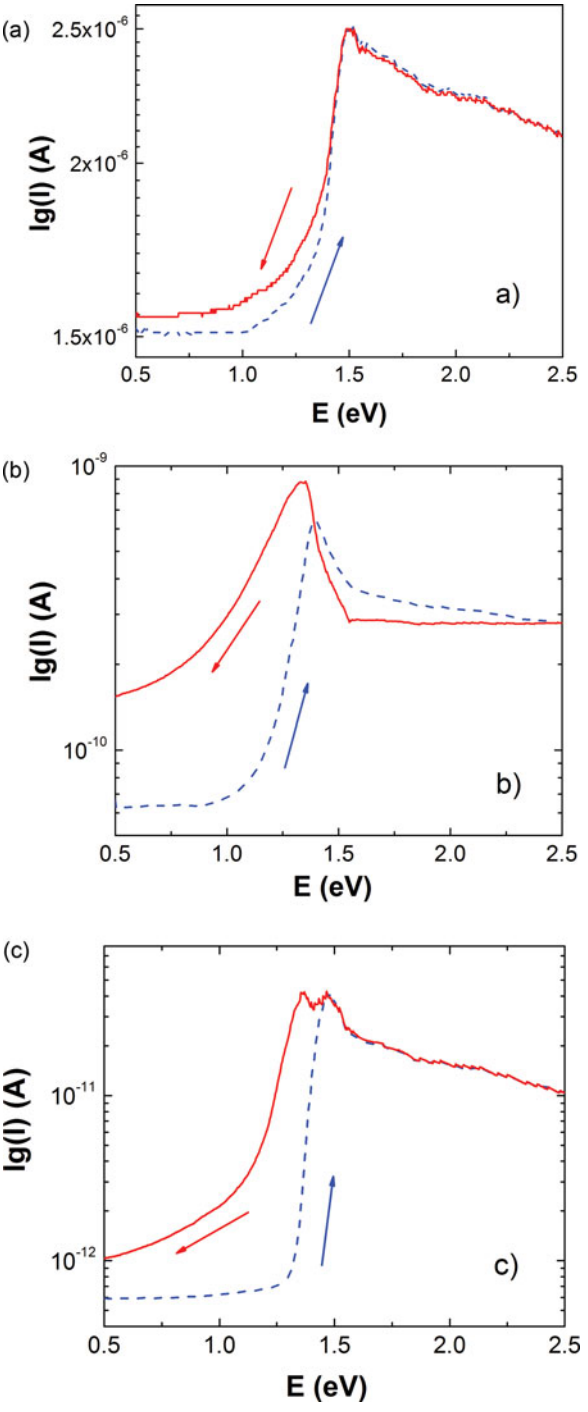

Figure 3. Spectral dependencies of the photocurrent of the $CuInS_2$-$ZnIn_2S_4$ crystals with 4 mol% (a), 8 mol% (b), and 12 mol% (c) of $ZnIn_2S_4$. Arrows indicate scanning directions of the spectra.

Table 3. Results of the EDX analysis of the samples

$ZnIn_2S_4$ content, mol%	Element	Measured concentration, at.%	Batch composition, at%
4	Cu	23.12 ± 0.45	23.30
	In	25.24 ± 0.23	25.24
	Zn	—	0.97
	S	51.65 ± 0.21	50.49
8	Cu	21.79 ± 0.34	21.70
	In	25.46 ± 0, 16	25.47
	Zn	1.76 ± 0.42	1.89
	S	50.99 ± 0.67	50.94
12	Cu	20.68 ± 0.54	20.17
	In	25.43 ± 0.36	25.69
	Zn	2.55 ± 0.32	2.76
	S	52.99 ± 0.77	51.38

the band-to-band generation. The shapes of the spectra are similar to that of $CuInS_2$ crystals, in which maxima appear at ~1.55 eV at 77 K [11]. This indicates that in the samples with as low 4 mol% of $ZnIn_2S_4$ effects of the cationic vacancies are minor. The drop of photoconductivity at the high energy side could be caused by the surface recombination. The effect of the surface recombination due to the high number of recombination centers at the surface is well described in, e.g., Refs. [12, 13].

By scanning the spectra from the low to high quantum energies the photoconductivity starts growing from ~1.1–1.2 eV. This evidences presence of the photoactive defect centers, from which carriers can be photogenerated. Meanwhile upon scanning from the high quantum energy, the enhanced persistent photoconductivity effect [12, 13] is induced. This phenomenon is still better expressed in the crystals containing 8 mol% of $ZnIn_2S_4$ as seen in Fig. 3(b). Moreover, an expressed feature of the crystals containing more $ZnIn_2S_4$ is a shift of the maxima positions towards lower energies (see Fig. 3(b, c)) and change of its amplitude (Fig. 3(b)) by scanning spectra from the higher energies. In Fig. 3(b) maximum appears at 1.4 eV by increasing quantum energy and at ~1.32 eV upon its decrease. In Fig. 3(c) the maxima appear at 1.47 eV and ~1.36 eV, respectively.

Such shift and light-induced enhanced photoconductivity can be attributed to the presence of two recombination centers with different capture cross-sections, i.e., different recombination rates [12, 13]. The model takes into account interaction of three defect centers with different parameters, namely, a) the so called r-centers, which act as slow recombination centers, b) fast recombination s-centers, and c) trapping t-centers [14]. The electron capture cross sections of recombination centers differ significantly: $S_{sn}/S_{rn} >> 10^3$. Meanwhile the trapping centers are located nearby the conductivity band, so they do not capture holes, assuring exchange of electrons only with the conductivity band. Though, such exchange results in the variation of the number of free electrons in the band. The trapped carriers are excluded from the transport, so sample conductivity might be significantly decreased. Furthermore, the filling of the trapping centers conditions also filling of both recombination centers, i.e., the shape of the photoconductivity spectra. In case carriers can recombine only through the slow r-centers, the photoconductivity would increase, i.e., the

enhanced photoconductivity is induced. This can be realized when the fast recombination s-centers become filled by the light generated carriers.

Thus, the photoconductivity maxima observed in Fig. 3 by increasing quantum energy are most probably caused by the photogeneration from r-centers created by copper vacancies V_{Cu}. In $CuInS_2$ compounds V_{Cu} levels have optical activation energies of about 0.1–0.2 eV [11, 15, 16]. For these defects the relation $S_{rn} << S_{rp}$ is fulfilled [11, 16], here S_{rp} is the hole capture cross section. Therefore electron recombination through these levels is slow and enhanced photoconductivity might be observed, if faster recombination centers become filled by the photogenerated carriers. Meanwhile s-centers could be created by Indium vacancies V_{In} or substitutional defects Cu_{In}. In $CuInS_2$ compounds these defects have activation energies of 0.18 eV and 0.22 eV, respectively [15, 16]; moreover, for these levels $S_{sn} \approx S_{sp}$ [16]. Therefore, upon light excitation, r-centers will be emptied from electrons, meanwhile s-centers become filled. Thus, by scanning the spectra down, position and amplitude of the maxima will change. The clear effect of V_S, V_{In} and/or Cu_{In} on the electrical properties of $CuInS_2$ was demonstrated also in Ref. [17]. The role of In defects was evidenced in [18]. The extensive data of defects in this material is presented in Ref. [19].

At low temperatures without excitation the shallow traps near the conductivity band are fully or partially emptied from electrons because of the compensating acceptors. The (self-) compensation effects of $CuInS_2$ were described also in Refs. [20, 21]. Therefore by scanning spectra up, photoconductivity is not observed, as electrons generated from s-centers into the conductivity band become captured by the shallow traps. In $CuInS_2$-$ZnIn_2S_4$ compounds such shallow donor traps might be formed by Sulfur vacancies V_S. In $CuInS_2$ two donor levels at ∼0.035 eV and ∼0.065-0.072 eV are caused by V_S [11, 15, 16, 20, 22]. Increase of the photoconductivity amplitude by scanning spectra down in Fig. 3(b) can be explained by the redistribution of electrons on defect levels and de-activation of the fast recombination center because of its filling.

Moreover, in Fig. 3(c), depicting compound with 12 mol% of $ZnIn_2S_4$, two distinctive photoconductivity maxima appear by scanning the spectra down. The induced maximum appears at ∼1.36 eV. Presumably this is because of the higher number of acceptors V_{Cu}, causing increased recombination probability for nonequilibrium electrons. Thus, after the preliminary light excitation, some electrons will still remain on r-centers, and their transitions to the conductivity band appear as the second high-energy maximum. The shift of the defect maxima towards the higher energies with increasing $ZnIn_2S_4$ content can be explained by the increase of the band gap width [23].

Investigations of the thermally stimulated current (TSC) spectra is the alternative and complementary tool for the photoelectrical spectroscopy. TSCs allow analysis of the thermal generation processes from the defect levels that might be optically inactive [24, 25]. Temperature dependencies of the electrical conductivity and TSCs were measured in the temperature region from ∼20 K up to 300 K in the dark and after the light pre-excitation at low temperatures, respectively. TSCs were calculated as the differences of the dark conductivity and conductivity measured after the light pre-excitation.

Temperature dependencies of the dark conductivity and TSCs are presented in Fig. 4. The dark conductivity dependencies are non-exponential, indicating the complex carrier thermal generation mechanism. With increasing $ZnIn_2S_4$ content, material conductivity decreases by many orders of magnitude (Fig. 3). This can be explained by the increasing role of the cationic vacancies, which are acceptors in chalcogenic compounds, compensating shallow donors. The intensification of their effect is seen in behavior of both defect-related and induced photoconductivity as described above.

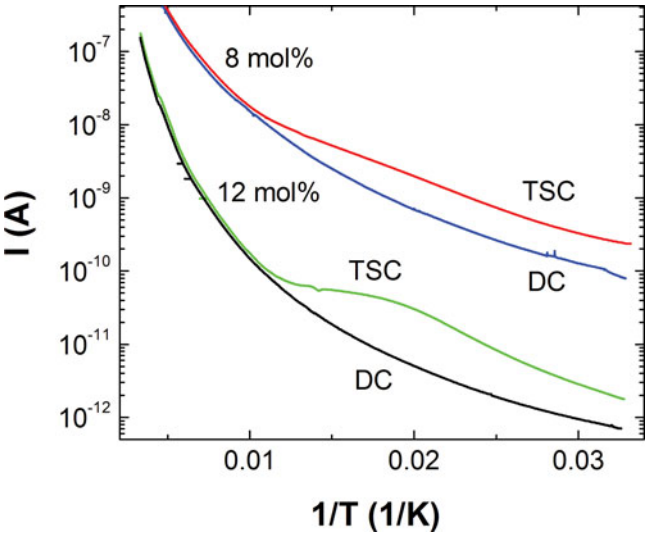

Figure 4. Temperature dependencies of the dark current (DC) and thermally stimulated current (TSC) in the crystals with 8 mol% and 12 mol% $ZnIn_2S_4$ as indicated on Fig.

To analyze the properties of the traps in materials in which enhanced photoconductivity was observed, TSC spectra were measured (see Figs. 4 and 5). The samples were photoexcited by the best absorbed light in order to fill the traps, i.e., t-levels by electrons. It can be seen in Fig. 5 that upon subtraction of the non-exponential dark current, linear parts in TSC appear in Arrhenius scaling.

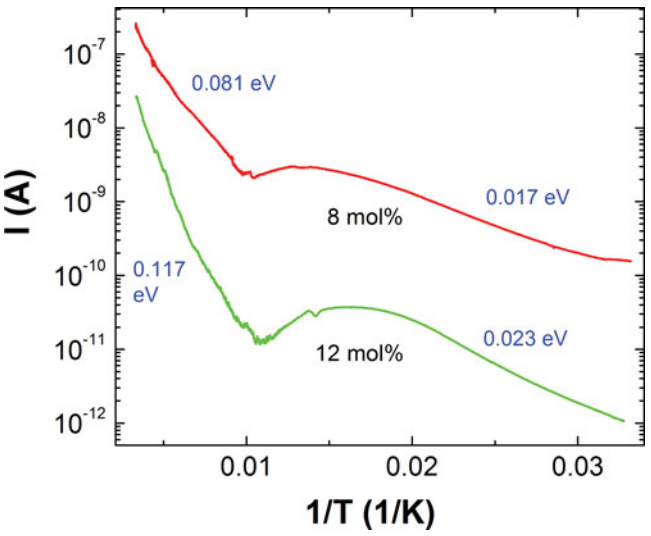

Figure 5. Temperature dependencies of the thermally stimulated current (TSC) with subtracted dark current in the crystals with 8 mol% and 12 mol% $ZnIn_2S_4$ as indicated on Fig. Numbers nearby the linear parts of the curves indicate the effective thermal activation energy values.

The first of them characterizes the well expressed trap-related maximum, and the second one is seen in the high temperature region. The maximum appears at about 70 K in the samples with 8 mol% of $ZnIn_2S$ and at about 80 K in the samples with 12 mol% of $ZnIn_2S$.

Their effective thermal activation energies are about 0.017 eV and 0.023 eV, respectively. They can be attributed to the generation of electrons from the shallow donor D_1. The current growth at the higher temperatures has the effective activation energy values of 0.081 eV and 0.117 eV, respectively. It can be caused by the jumps from the donor state D_2. Both the shift of the maxima temperature and increase of the thermal activation energy values with increasing $ZnIn_2S$ content could be due to the increasing bandgap width, as stated above. On the other hand, both the non-exponential current growth and low activation energy values could also be related to sample inhomogeneity, causing appearance of potential fluctuations of the band gap edges [26–29].

3. Summary and Conclusions

The horizontal Bridgman–Stockbarger method was used to grow $CuInS_2$-$ZnIn_2S_4$ solid solutions with different contents of $ZnIn_2S_4$, ranging from 4 to 16 mol%. The samples had demonstrated n-type electrical conductivity. The X-Ray analysis was applied to reveal their structural properties. In 4*a* (0,0,0) crystallographic position the heterovalent substitution of Cu atoms by Zn atoms was found with one divalent Zn atom replacing two univalent Cu atoms. Thus, the vacancy type cationic defects within the chalcopyrite structure are formed, the density of which is proportional to the density of Zn atoms. The photoelectrical properties of materials were investigated by the spectral dependencies of photoconductivity at ∼30 K. Appearance of the induced photoconductivity effect in $CuInS_2$-$ZnIn_2S_4$ solid solutions having 8 to 12 mol% of $ZnIn_2S_4$ was demonstrated. It could be explained by the model of two recombination centers with different capture cross sections. The effect is presumably related with the vacancy defect centers V_{Cu}, V_{In} or substitutional defect Cu_{In} levels. The first of these defects acts as the slow recombination center, meanwhile the latter two are the fast recombination centers. Measurements of the temperature dependencies of electrical conductivity and thermally stimulated currents confirmed the presence of the electrically active shallow defects.

Funding

The partial financial support from the Research Council of Lithuania (Project No TAP LU 02/2014) and the State Agency on Science, Innovations and Informatization of Ukraine is acknowledged.

References

[1] Scheer, R., Walter, T., Schoock, H. W., Fearheiley, M. L., & Lewerenz, H. J. (1993). *Appl. Phys. Lett.*, *63*, 3294.

[2] Ahn, S. J., Kim, C. W., Yun, J. H., Gwak, J., Jeong, S., Ryu, B.-H., & Yoon, K. H. (2010). *J. Phys. Chem. C*, *114*, 8108.

[3] Siemer, K., Klaer, J., Luck, I., Bruns, J., Klenk, R., & Braunig, D. (2001). *Sol. Energy Mater. Sol. Cells*, *67*, 159.

[4] Klaer, J., Bruns, J., Henninger, R., Siemer, K., Klenk, R., Ellmer, K., & Braunig, J. (1998). *Semicond. Sci. Technol.*, *13*, 1456.

[5] Klenk, R., Klaer, J., Scheer, R., Lux-Steiner, M. C., Luck, I., Meyer, N., & Ruehle, U. (2005). *Thin Solid Films*, *480* (SI), 509.
[6] Akselrud, L. G., Zavalij, P. Yu., Grin', Yu. N., Pecharsky, V. K., Baumgartner, B., & Wolfel, E. (1993). *Mater. Sci. Forum*, *133-136*, 335.
[7] Wiberg, N. (1995). *Lehrbuch der Anorganischen Chemie*, Walter de Gruyter, Berlin.
[8] Yamamoto, T., Luck, I. V., & Scheer, R. (2000). *Appl. Surf. Sci.*, *159*, 350.
[9] Romanyuk, Y. E., Yu, K. M., Walukiewicz, W., Lavrynyuk, Z. V., Pekhnyo, V. I., & Parasyuk, O. V. (2008). *Sol. Energy Mater. Sol. Cells*, *92*, 1495.
[10] Parasyuk, O. V., Lavrynyuk, Z. V., Zmiy, O. F., & Romanyuk, Y. E. (2009). *J. Cryst. Growth.*, *311*, 20381.
[11] Ivanov, V. A., Viktorov, I. A., & Gremenok, V. F. (2002). *Technical Phys.*, *47*, 1197.
[12] Bube, R. H. (1960). *Photoconductivity of Solids*, John Wiley and Sons, New York.
[13] Ryvkin, S. M. (1963). *Photoelectrical Phenomena in Semiconductors*, Fizmatgiz, Moscow (In Russian).
[14] Lashkarev, V. E., Liubchenko, A. V., & Sheinkman, M. K. (1981). *Nonequilibrium Phenomena in Photoconductors*, Naukova Dumka, Kiev (In Russian).
[15] Binsma, J. J. M. (1983). *J. Phys. Chem. Solids.*, *44*, 237.
[16] Onishi, T., Abe, K., Miyoshi, Y., Wakita, K., Sato, N., & Mochizuki, K. (2005). *J. Phys. Chem. Sol.*, *66*, 1947.
[17] Yoshino, K., Nomoto, K., Kinoshita, A., Ikari, T., Akaki, Y., & Yoshitake, T. (2008). *J. Mater. Sci: Mater. Electron.*, *19*, 301.
[18] Ueng, H. Y., and Hwang, H. L. (1990). *J. Phys. Chem. Sol.*, *51*, 10.
[19] Copper indium sulfide (roquesite, CuInS2) impurities and defects. (2000). *In: Landolt-Börnstein - Group III Condensed Matter. Numerical Data and Functional Relationships in Science and Technology. Vol 41E: Ternary Compounds, Organic Semiconductors*. Eds.: Madelung, O., Rössler, U., and Schulz, M., Springer: Berlin.
[20] Ueng, H. Y. & Hwang, H. L. (1989). *J. Phys. Chem. Sol.*, *50*, 1297.
[21] Yamamoto, T., Luck, I. V., Scheer, R., & Katayama-Yoshida, H. (1999). *Physica B 273-274*, 927.
[22] Van Gheluwe, J., Versluys, J., Poelman, D., Verschraegen, J., Burgelman, M., & Clauws, P. (2006). *Thin Solid Films*, *511*, 304.
[23] Davidyuk, G. E., Bozhko, V. V., Novosad, O. V., Kozer, V. R., & Parasyuk, O. V. (2009). Sci. Bul. Volyn Lesya Ukrainka Nat. *Univ.: Physical Sciences 18*, 19 (In Ukrainian).
[24] Kažukauskas, V. & Kiliulis, R. (1993). *Phys. Status Solidi B*, *179*, K21.
[25] Kiliulis, R., Kažukauskas, V., & Bourgoin, J. C. (1996). *J. Appl. Phys.*, *79*, 6951.
[26] Sheinkman, M. K. & Shik, A. J. (1976). *Phys. Tekh. Polupr.*, *10*, 209 (in Russian).
[27] Vaitkus, J., Kažukauskas, V., Kiliulis, R., & Storasta, J. (1994). *Inst. Phys. Conf. Series*, *136*, 755.
[28] Kažukauskas, V., Kuehnel, G., & Siegel, W. (1997). *Appl. Phys. Lett.*, *70*, 1751.
[29] Kažukauskas, V. (1998). *J. Appl. Phys.*, *84*, 2053.